LANGMUIR Article
Cite This: Langmuir 2018, 34, 15578−15586
pubs.acs.org/Langmuir

Photo-Oxidation of Unilamellar Vesicles by a Lipophilic Pterin: Deciphering Biomembrane Photodamage

Mariana Vignoni,[†] Maria Noel Urrutia,[†] Helena C. Junqueira,[‡] Alexander Greer,[§,∥] Ana Reis,[⊥] Mauricio S. Baptista,[‡] Rosangela Itri,[*,#] and Andrés H. Thomas[*,†]

[†]Instituto de Investigaciones Fisicoquímicas Teóricas y Aplicadas, Dep. de Química, Fac. de Cs. Exactas, Universidad Nacional de La Plata, CCT La Plata-CONICET, CC 16, Suc. 4, 1900 La Plata, Argentina

[‡]Departamento de Bioquímica, Instituto de Química, Universidade de São Paulo, 05508-000 São Paulo, Brazil

[§]Department of Chemistry, Brooklyn College, City University of New York, Brooklyn, 11210 New York, United States

[∥]Ph.D. Program in Chemistry, The Graduate Center of the City University of New York, 365 Fifth Avenue, 10016 New York, New York, United States

[⊥]ICETA/REQUIMTE/LAQV, Department of Chemistry and Biochemistry, Faculty of Sciences, University of Porto, 4169-007 Porto, Portugal

[#]Institute of Physics, University of São Paulo, 05508-090 São Paulo, Brazil

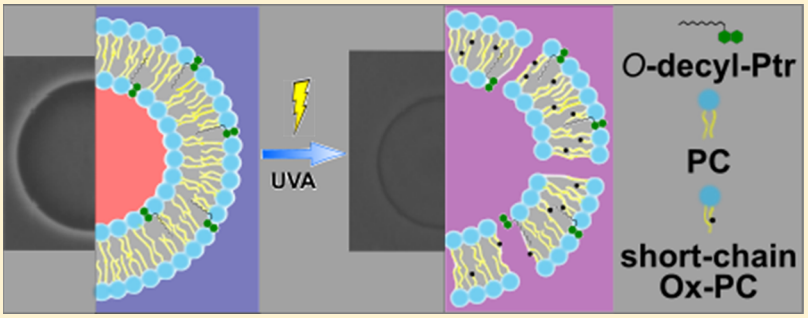

ABSTRACT: Pterins are natural products that can photosensitize the oxidation of DNA, proteins, and phospholipids. Recently, a new series of decyl-chain (i.e., lipophilic) pterins were synthesized and their photophysical properties were investigated. These decyl-pterins led to efficient intercalation in large unilamellar vesicles and produced, under UVA irradiation, singlet molecular oxygen, a highly oxidative species that react with polyunsaturated fatty acids (PUFAs) to form hydroperoxides. Here, we demonstrate that the association of 4-(decyloxy)pteridin-2-amine (*O*-decyl-Ptr) to lipid membranes is key to its ability to trigger phospholipid oxidation in unilamellar vesicles of phosphatidylcholine rich in PUFAs used as model biomembranes. Our results show that *O*-decyl-Ptr is at least 1 order of magnitude more efficient photosensitizer of lipids than pterin (Ptr), the unsubstituted derivative of the pterin family, which is more hydrophilic and freely passes across lipid membranes. Lipid peroxidation photosensitized by *O*-decyl-Ptr was detected by the formation of conjugated dienes and oxidized lipids, such as hydroxy and hydroperoxide derivatives. These primary products undergo a rapid conversion into short-chain secondary products by cleavage of the fatty-acid chains, some of which are due to subsequent photosensitized reactions. As a consequence, a fast increase in membrane permeability is observed. Therefore, lipid oxidation induced by *O*-decyl-Ptr could promote cell photodamage due to the biomembrane integrity loss, which in turn may trigger cell death.

INTRODUCTION

Oxidative stress can generate lipid peroxidation during many physiological and pathological processes.[1−3] Light accelerates lipid peroxidation quite substantially, being critical to explain damage in the photosynthetic apparatus, food oxidation, skin photodamage, as well as the success of a clinical modality of treating cancerous and infectious diseases called photodynamic therapy (PDT).[4−6] Endogenous or exogenous photosensitizers act through two different mechanisms: reactions where the generation of radicals takes place via a direct contact reaction with the target molecule through electron transfer or hydrogen abstraction (type I mechanism), and reactions where singlet oxygen ($^1O_2$) is produced by energy transfer from the triplet state of the photosensitizer (type II mechanism).[7,8] The role and the importance played by each of these mechanisms is critical to allow improvement in the methodologies to avoid or catalyze light-induced peroxidation reactions.

Lipophilic photosensitizers are reported to interact or intercalate with biomembranes, which usually increases its efficiency in photodamage.[9−12] For instance, photosensitizing

Received: September 28, 2018
Revised: November 19, 2018
Published: November 20, 2018

DOI: 10.1021/acs.langmuir.8b03302
Langmuir 2018, 34, 15578−15586

properties of porphyrins and chlorins with different substituents showed their dependence with the position and depth in the lipid membrane.[13,14] In addition, a lipophilic photosensitizer such as chlorophyll *a* photoinduces membrane damage in giant unilamellar vesicles (GUVs), while no damage was observed when a hydrophilic photosensitizer, riboflavin, was used.[15] Moreover, photoinduced bactericidal activity is enhanced when polycationic porphyrins have a hydrophobic alkyl chain incorporated.[16] The main reasons for the impressive increase in photosensitizer efficiency upon membrane binding were recently described by Bacellar et al.[17] by comparing two PDT phenothiazium cation photosensitizers. These authors showed that the key step that permits membrane leakage is caused by direct contact reactions between the photosensitizer and either the lipid double bond or the lipid hydroperoxide, which is previously formed by the ene-reaction with singlet oxygen. However, there is no report in the literature performing such analysis for natural photosensitizers. This knowledge is fundamental to understand a whole range of effects related with light-induced lipid photooxidation triggered by compounds normally found in photosynthetic organisms as well as in the skin or in food.

Pterins, heterocyclic compounds derived from 2-aminopteridin-4-(3*H*)-one,[18] are present in biological systems in multiple forms, and play different roles ranging from pigments to enzymatic cofactors for numerous redox and one-carbon transfer reactions.[19,20] In particular, 5,6,7,8-tetrahydrobiopterin is an essential cofactor for aromatic amino acid hydroxylases[21] and participates in the regulation of melanin biosynthesis.[22] Unconjugated oxidized pterins are photochemically reactive[23] and accumulate in human skin under pathological conditions.[24] These compounds absorb UVA radiation (320−400 nm), fluoresce, undergo photo-oxidation, and generate reactive oxygen species.[23] Moreover, they can act as photosensitizers through both type I and type II mechanisms, inducing damage to proteins[25] and DNA,[26−28] and also inactivation of enzymes[29] and bacteria.[30]

It was recently demonstrated that pterin (Ptr, parent and unsubstituted compound of oxidized pterins) (Figure 1) can photoinduce oxidation of lipids in membranes of large unilamellar vesicles (LUVs).[31] Conjugation of a decyl-chain to the pterin moiety dramatically increases its solubility in common organic solvents and also enables its facile intercalation in LUVs.[32,33] In addition, decyl-pterins present a more efficient intersystem crossing to the triplet excited state as compared to Ptr, showing higher $^1O_2$ quantum yields (Φ_Δ), which implies a greater photo-oxidative activity. Previous work suggested a potential use of alkyl-pterins as photosensitizers in biomembranes.[32]

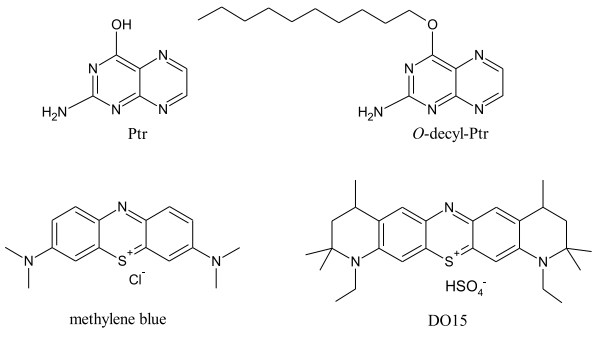

Figure 1. Chemical structure of Ptr, *O*-decyl-Ptr, methylene blue and DO15.

In this work, we use decyl-pterins to understand the mechanisms by which lipophilic derivatives of natural photosensitizers cause definitive damage in lipid membranes. Among the four alkyl-pterin derivatives described in ref 32, we chose 4-(decyloxy)pteridin-2-amine (*O*-decyl-Ptr) (Figure 1), because it was the compound with the highest Φ_Δ value. Here, we describe the association of *O*-decyl-Ptr to lipid membranes and its ability to trigger phospholipid oxidation. LUVs and GUVs rich in polyunsaturated fatty acids (PUFAs) were investigated and the results were compared to those obtained with Ptr, which is a more hydrophilic photosensitizer. We will show that the damaging processes that lead to membrane pores for the *O*-decyl-Ptr photosensitizer turn out to be similar to the processes recently described by a lipophilic methylene blue derivative (DO15) (Figure 1),[17] but there are some interesting differences. Even though lipid hydroperoxides are initially formed during photosensitized oxidation by *O*-decyl-Ptr, they do not accumulate in the membranes as in the case of DO15. The formation of shortened lipid tails arises as a consequence of secondary processes leading to increased membrane permeability, as key compounds in the membrane photoresponse to oxidative stress.

EXPERIMENTAL SECTION

Chemicals. Ptr (purity > 99%) was purchased from Schircks Laboratories (Switzerland). *O*-Decyl-Ptr was synthesized as previously reported.[32] 1,2-Dilinoleoyl-*sn*-glycero-3-phosphocholine (DLPC, ≥99%, powder) and 1,2-dioleoyl-*sn*-glycero-3-phosphocholine (DOPC, ≥99%, powder) were obtained from Avanti Polar Lipids Inc. L-α-Soybean phosphatidylcholine (SoyPC, ≥99% (TLC), lyophilized powder), 3,5-di-*tert*-4-butylhydroxytoluene (BHT), 5(6)-carboxyfluorescein (CF), xylenol orange (XO), Triton X-100 and Sephadex G-50 were bought from Sigma-Aldrich. Tris-(hydroxymethyl)aminomethane (Tris) was acquired by Genbiotech. Sodium chloride was from Cicarelli, ammonium iron(II) sulfate hexahydrate from Carlo Erba and sulfuric acid (95−98% RA) from Anedra. HPLC grade chloroform and methanol were purchased from U.V.E. and J. T. Baker, respectively. Purified water from a Milli-Q reagent water system apparatus was used.

Absorption Measurements. Absorption spectra were obtained from a Shimadzu UV-1800 spectrophotometer. 0.4 or 1 cm optical path length quartz cells were used.

Fluorescence Measurements. Steady-state fluorescence measurements were obtained with a single-photon-counting equipment FL3TCSPC-SP (HORIBA Jobin Yvon), described elsewhere.[34]

Steady-State Irradiation. LUVs' irradiation was carried out in quartz cells. The radiation source employed were Rayonet RPR 3500 lamps (Southern N.E. Ultraviolet Co.) with emission centered at λ = 350 nm [band width (fwhm) 20 nm]. Aqueous dispersions were irradiated using one lamp in all experiments, except in the mass spectrometry (MS) analysis in which two lamps were employed. The incident photon flux density ($q_{n,p}^{0V}$) for each lamp was measured using Aberchrome 540 (Aberchromics Ltd.) as an actinometer.[35] The obtained value was 9.9 (±0.2) × 10^{-6} einstein L^{-1} s^{-1}.

Preparation of LUVs. LUVs were prepared using chloroform solutions of lipids (DOPC, DLPC, and SoyPC), dried under nitrogen stream and hydrated in Tris buffer (20 mM, pH 7.4). Samples were vortexed for several minutes, followed by extrusion through a 100 nm porous membrane (Avanti Polar). LUVs were kept at 4 °C prior to use. Dynamic light scattering measurements were performed with a Malvern Zetasizer Nano-ZS to estimate the size of the LUVs formed. Results showed a diameter of 138 ± 10 nm [mean ± standard deviation (SD), triplicates]. The polidispersity index was 0.12.

LUVs Binding Experiments. Experiments were performed as previously described.[32] Briefly, kinetic experiments were performed to

DOI: 10.1021/acs.langmuir.8b03302
Langmuir 2018, 34, 15578−15586

ensure equilibrium conditions, which were reached in 10 min, because no further increase in fluorescence was observed after that time. A titration method was then used to determine the binding constant (K_b).[36] Increasing quantities of lipid LUVs were added to a Tris solution of *O*-decyl-Ptr (2 μM). The samples were excited at 340 nm and corrected fluorescence spectra were recorded between λ = 390 and 600 nm. Total fluorescence intensities (F) were calculated by the integration of the fluorescence band between λ = 410 and 600 nm. F was plotted on a graph against the lipid concentration and the following equation was used to fit the data

$$F_L = F_0 + (F_\infty - F_0) \times [L]/(1/K_b + [L]) \quad (1)$$

where the three values F_0, F_L, and F_∞ are the fluorescence intensities of the compound without lipid, with lipid at concentration L, and that which would be obtained asymptotically at complete binding, respectively; and [L] is the lipid concentration.

FOX 2 Assay. Experiments were performed according to the procedure described by Wolff with some modifications.[37] The method is based on the oxidation of ferrous to ferric ions by hydroperoxides (eq 2), which react with XO to form a colored complex (eq 3).

$$ROOH + Fe^{2+} \rightarrow Fe^{3+} + RO^{\bullet} + OH^{-} \quad (2)$$

$$Fe^{3+} + XO \rightarrow \text{blue-purple complex} \quad (3)$$

The reagent was prepared as follows: 250 μM $(NH_4)_2Fe(SO_4)_2 \cdot 6H_2O$ (9.8 mg) and 25 mM H_2SO_4 (139 μL) were dissolved in 5 mL of water, mixed with 4 mM BHT (88.2 mg), 100 μM XO (7.2 mg), and 45 mL of methanol. Afterward, another 45 mL of methanol and 5 mL of water were added. For the experiment, aliquots of 50 μL of samples were added to 950 μL of FOX 2 reagent in microtubes, homogenized in a vortex mixer and left to react for 30 min in the dark at room temperature. After incubation, the absorbance of samples was read between 200 and 700 nm. As the extinction coefficient of the Fe/XO complex may differ depending on the acid used, pH, solvents and with the nature of hydroperoxides, concentrations of lipid hydroperoxides were calculated as mM H_2O_2 equivalents based on a standard curve spanning a 0–0.4 mM H_2O_2 range (r^2 0.9704), which were prepared and subjected to the same treatment of the studied samples.

Photoinduced CF Release from LUVs. LUVs were prepared as described above, but for hydration, 500 μL of 50 mM CF in 10 mM Tris buffer was used, generating a LUV suspension with CF encapsulated in the inner compartment. Using a Sephadex G-50 exclusion chromatography column (1 × 15 cm) with 0.3 M NaCl in 10 mM Tris buffer as eluent, free CF was removed and the fraction containing LUVs was collected.[38] The high CF amounts inside LUVs results in fluorescence self-quenching, therefore an increase in CF fluorescence points out membrane damage and leakage of CF to the outer solution.[39] Membrane damage quantification was performed using a fluorescence quartz cell of 0.4 × 1 cm. The final volume was 800 μL in 0.3 M NaCl–10 mM Tris buffer, adding 20 μL of lipid suspension. The concentration of the photosensitizer was 5 μM, except for the control which had no compound. The irradiation was performed as described above. Fluorescence spectra were recorded between λ = 500 and 680 nm and were monitored as function of irradiation, with excitation at λ = 480 nm. Triton X-100 was added at the end of the experiment, and the fluorescence was recorded. To calculate the percent of released CF, the following equation was used

$$\%\ CF_{released} = 100\%(F - F_0)/(F_T - F_0) \quad (4)$$

where F_0 is the initial fluorescence intensity, F is the fluorescence intensity at each irradiation time and F_T is the total fluorescence intensity after membrane disruption with Triton X-100.

Preparation of GUVs. GUVs of DLPC were prepared by the electroformation method.[40] Briefly, lipids dissolved in chloroform (10 μL, 1 mg/mL) were dispersed over glass surfaces coated with fluor tin oxide, and were then placed with their conductive sides facing one another using a 2 mm thick Teflon spacer. This chamber was filled with solutions of 0.2 M sucrose and then connected to an alternating power generator (Minipa MFG-4201A; Korea) at 10 Hz frequency and 1.5 V for 1.5–2 h at room temperature. Afterward, vesicles were transferred to an Eppendorf vial and kept at 4 °C. For the experiment, 100 μL of the GUVs was diluted with 600 μL of a 0.2 M glucose solution and added to an observation chamber. This produced a sugar asymmetry between the outer and the inner vesicle environment. Sugar solutions' osmolarities were measured with a cryoscopic osmometer Osmomat 030 (Gonotec, Germany) and prudently matched to avoid osmotic pressure effects. The small density difference between the inner and outer solutions drives the vesicles to the bottom slide where they can be observed. Moreover, the refractive index difference between both sugar solutions offers a better optical contrast when observing the vesicles with phase contrast microscopy.

To study GUVs photodamage, the photosensitizers were dissolved in the glucose solution and the procedure described previously was followed. The concentration of the photosensitizers was calculated for the final solution in the observation chamber amounting to 5 μM.

Optical Microscopy. An inverted microscope was used in this study (Axiovert 200, Carl Zeiss; Germany) with a Ph2 63 objective. Images were obtained with an AxioCam HSm, Carl Zeiss. To observe the vesicles, the transmission mode (bright field) was used. Under these conditions, vesicles in the presence of the photosensitizer suffered no changes for at least 1 h of observation. The samples were irradiated with the 103 W Hg lamp (HXP 120, Kubler, Carl Zeiss, Germany) of the microscope employing a proper filter for photoactivation of pterin derivatives (λ_{ex} = 325–375 nm; beam split 400 nm; λ_{em} = LP 420 nm). Optical phase contrast fading with time irradiation was analyzed by taking into account the decrease of brightness level intensity using the Image J software.

Lipid Extraction. Lipids were extracted from the reaction mixture using a modified procedure of the Bligh–Dyer method[41] (with previously addition of 0.01% BHT, w/v), which is described in ref 31.

MS Experiments. The liquid chromatography equipment coupled to the MS (LC–MS) system was equipped with an UPLC chromatograph (ACQUITY UPLC, Waters), and a UV–vis detector (Acquity TUV), coupled to a quadrupole time-of-flight mass spectrometer (Xevo G2-QTof-MS, Waters) (UPLC-QTof-MS), equipped with an electrospray ionization source. UPLC analyses were performed using an Acquity UPLC BEH C8 (1.7 mm; 2.1 × 50 mm) column (Waters), with a mobile phase of ammonium acetate 8 mM (solvent A) and methanol (solvent B), programmed as follows: 86% solvent B for 3 min, followed by a linear increase to 95% solvent B at 10 min held for 6 min. After 16 min, the mobile phase was returned to initial conditions (3 min). The flow rate was 0.45 mL min^{-1}. The QTof-MS was operated in the positive-ion mode with a capillary voltage of 2.5 kV, the cone voltage of 50 V, the cone gas flow of 20 L/h, the source temperature set to 130 °C and the desolvation temperature set to 450 °C. For the tandem MS experiments the collision energies varied between 15 and 35 eV. The scan range was from 50 to 1000 atomic mass units (amu). For high mass accuracy, the Q-Tof was calibrated using 0.5 mM sodium formate in 50:50 H_2O/acetonitrile (vol/vol). The instrument drift was compensated by applying a lockmass correction.

RESULTS AND DISCUSSION

Interaction Studies with Model Membranes. Decyl-pterins were previously found to interact with lipid membranes with binding constants (K_b) of about 10^4 M^{-1}, as previously described.[32] This is an impressive increase in the level of membrane interaction compared with the pure Ptr moiety.[31] As the binding of a compound to the membrane depends on the lipid composition of the LUVs,[42] here we expand on the work and determined the K_b values of *O*-decyl-Ptr for LUVs formed from SoyPC, DOPC, and DLPC. The fluorescence spectra of samples with the same concentration of *O*-decyl-Ptr and increasing concentration of a given lipid were recorded and the fluorescence intensity as a function of the

DOI: 10.1021/acs.langmuir.8b03302
Langmuir 2018, 34, 15578–15586

concentration of lipid was fitted with eq 1. K_b values for the binding of *O*-decyl-Ptr to LUVs were determined to be 3 (±1) × 10^4 M^{-1}, 4 (±1) × 10^4 M^{-1} and 7 (±2) × 10^4 M^{-1}, for DOPC, DLPC, and SoyPC, respectively. These values were similar to that obtained earlier for EggPC [4 (±1) × 10^4 M^{-1}].

Note that all the lipids studied present the same phosphocholine polar head, but differ in the alkyl chain composition, regarding the number of chain unsaturation. The fact that all the obtained K_b values were similar, points out that the hydrophobicity of the photosensitizer plays indeed an important role in the photosensitizer−membrane interaction. It is also important to mention that the small but representative increase in K_b from DOPC to SoyPC points to the increased photosensitizer membrane affinity with the increment in lipid unsaturation, indicating that van der Walls interactions between the photosensitizer and the lipid double bond are involved in the interaction and suggesting that the chromophore unit of the photosensitizer has some level of direct contact with the lipid double bonds.

Photosensitized Lipid Peroxidation of LUVs. Ptr crosses the lipid membrane and does not intercalate, though it still produces lipid peroxidation by photosensitization.[31] Knowing that *O*-decyl-Ptr interacts with membranes with significant K_b values, photosensitized lipid peroxidation is hypothesized to be more effective. Therefore, SoyPC LUVs containing 2% mol of the photosensitizer were exposed to UVA radiation for different periods of time and the treated samples were analyzed with different techniques to evaluate lipid peroxidation.

A useful tool for an initial assessment of lipid peroxidation is to investigate the formation of conjugated dienes and trienes.[43−45] Therefore, samples were first analyzed by UV−vis spectrophotometry and the absorbance at 234 nm, where conjugated dienes absorb, was monitored. As shown in Figure 2a, the formation of conjugated dienes in SoyPC LUVs was much faster using *O*-decyl-Ptr than using Ptr. Actually, under the experimental conditions used and in the period of time analyzed, the formation of conjugated dienes by Ptr was almost negligible. The same behavior was observed when the time evolution of the absorbance at 270 nm, where conjugated trienes absorb, was analyzed as a function of irradiation time (Figure 2b). Undoubtedly, only when *O*-decyl-Ptr is employed as a photosensitizer, conjugated trienes are formed in this period of time. In addition, as expected, in controls of nonirradiated SoyPC LUVs with and without photosensitizers, no significant conjugated dienes and trienes were observed.

Another generic marker of lipid peroxidation, FOX 2 assay (ferrous iron/XO II),[46] provided a similar response. Figure 3 shows that the amount of lipid hydroperoxides produced in the presence of *O*-decyl-Ptr was much higher than in the presence of Ptr, the latter being very similar to the lipid hydroperoxides obtained when no photosensitizer was present. Control experiments without irradiation showed no increase in lipid hydroperoxides over time.

The results shown here clearly demonstrated that *O*-decyl-Ptr is able to photoinduce lipid peroxidation and that this process is much faster than that observed for free Ptr, thus indicating that the intercalation of the alkyl-pterins to the membrane enhances the photosensitized reactions. This is in agreement with several other reports in the literature pointing to the fact that membrane insertion is key to cause definitive membrane damage.[15,17] Taking into account only the photosensitizing properties of pterins,[47] both type I and type II

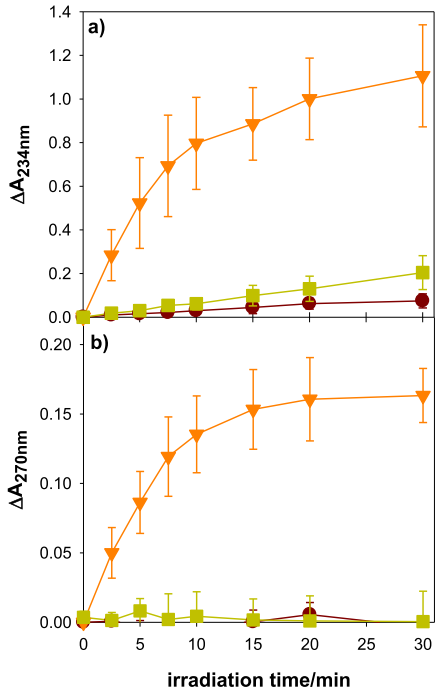

Figure 2. Formation of conjugated dienes (a) and trienes (b) in SoyPC LUVs, upon UVA irradiation, with *O*-decyl-Ptr (orange down-pointing triangle), Ptr (yellow square) and without the photosensitizer (brown circle). Error bars correspond to SD from 3 different experiments.

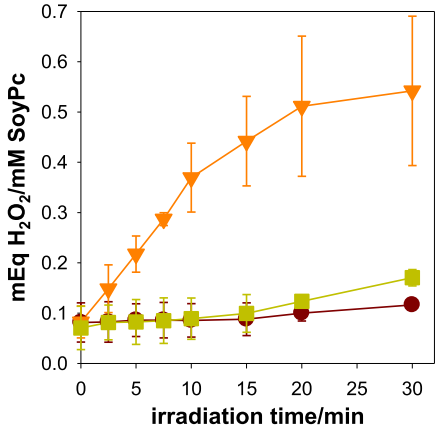

Figure 3. FOX 2 assay in SoyPC LUVs irradiated in the presence of with *O*-decyl-Ptr (orange down-pointing triangle), Ptr (yellow square) and without photosensitizer (brown circle). Error bars correspond to SD from 2 to 3 different experiments.

mechanisms may be involved in the initiation of the lipid peroxidation photoinduced by *O*-decyl-Ptr. However, considering also that singlet oxygen can diffuse and has an action pathway of around 100 nm in water,[17] would be hard to explain why a photosensitizer binding to a 5 nm structure would be so important to cause damage. Indeed, these data points to the importance of the reaction that depends on the contact between the photosensitizer and the lipid double bond.

Analysis of Photoproducts by MS. To gain an insight into the structural characteristics of the products formed by photosensitization with *O*-decyl-Ptr, lipid extracts were analyzed by the UPLC equipment coupled to a mass spectrometer. In this case, and to simplify the analysis of the

DOI: 10.1021/acs.langmuir.8b03302
Langmuir 2018, 34, 15578−15586

Table 1. Molecular Formula, Observed and Calculated Mass and Mass Error of DLPC Long-Chain Oxidized Products Detected in LC−MS Spectra

	molecular formula	observed mass	calculated mass	error (ppm)	error (mDa)
DLPC (18:2/18:2)	$C_{44}H_{81}NO_8P^+$	782.5716	782.5694	2.1	1.6
+O	$C_{44}H_{81}NO_9P^+$	798.5634	798.5643	−1.9	−1.5
+2O	$C_{44}H_{81}NO_{10}P^+$	814.5589	814.5593	−1.1	−0.9
+3O	$C_{44}H_{81}NO_{11}P^+$	830.5527	830.5542	−2.4	−2.0
+4O	$C_{44}H_{81}NO_{12}P^+$	846.5475	846.5491	−2.5	−2.1
−2H	$C_{44}H_{79}NO_8P^+$	780.5539	780.5538	0.7	0.5
+O − 2H	$C_{44}H_{79}NO_9P^+$	796.5444	796.5487	−6.1	−4.8
+2O − 2H	$C_{44}H_{79}NO_{10}P^+$	812.5425	812.5436	−2.0	−1.6
+3O − 2H	$C_{44}H_{79}NO_{11}P^+$	828.5359	828.5385	−3.8	−3.2
+4O − 2H	$C_{44}H_{79}NO_{12}P^+$	844.5339	844.5334	0.1	0.1

products, LUVs of DLPC (PC 18:2/18:2) were used. Irradiated DLPC LUVs with and without photosensitizer were analyzed after lipid extraction.

Before irradiation of DLPC LUVs, the LC−MS chromatograms showed a main peak and the corresponding mass spectrum recorded for this peak showed a $[M + H]^+$ ion at m/z 782.5716 (M = DLPC). After irradiation, several new peaks were observed in the chromatograms with retention times (t_R) lower than that of unmodified DLPC. LC−MS spectra recorded at different t_R showed several products with higher m/z values, corresponding to DLPC-oxidized phospholipids that have incorporated oxygen atoms (n = 1−4) to the hydrocarbon chains of the unsaturated fatty acids. The incorporation of one oxygen atom indicates that a hydroxy derivative was formed, as well as incorporation of two oxygen atoms could correspond to one hydroperoxide or two hydroxy groups, as reported earlier.[48] On the other hand, the incorporation of oxygen atoms with the loss of two H, corresponds to the formation of keto derivatives. The elemental compositions of products [M + nO] or [M + nO − 2H], where M is the elemental composition of DLPC, are listed in Table 1.

The extracted ion LC−MS chromatograms (XIC) of specific ions in irradiated solutions were registered. In the case of m/z 798, corresponding to products [M + O], two peaks corresponding to positional isomers, were registered whose area increased as a function of irradiation time (Figure 4a), thus suggesting the fast production of hydroxy derivatives. As previously described, these hydroxy derivatives are one of the end points of the peroxidation reactions and are formed by decomposition of hydroperoxides to peroxides and then to hydroxy derivatives (Scheme 1).[3]

The XIC of the ion at m/z 814 corresponding to [M + 2O] shows two chromatographic peaks before irradiation and four in the irradiated LUVs samples. LC−MS/MS analysis of the four products allowed the distinction of hydroperoxides derivatives from dihydroxy derivatives by the loss of H_2O_2 (−34 amu) from the precursor ion (m/z 814). Consequently, the presence of the two compounds detected in the sample before irradiation indicates the presence of some hydroperoxides produced by autooxidation reaction, whereas the products present only on the treated samples were dihydroxy derivatives. Peak intensities revealed that the two hydroperoxides increased their concentrations in the first minutes of irradiation and then showed a relatively slow consumption. On the other hand, the two dihydroxy derivatives rapidly increased their intensity and then reached a plateau (Figure 4b).

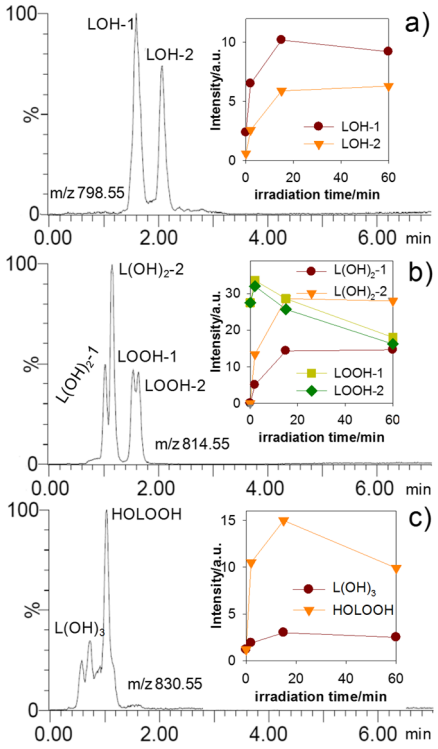

Figure 4. Extracted ion LC−MS chromatograms from oxidized products (a) m/z 798.55, (b) m/z 814.55, and (c) m/z 830.55. Insets: Time evolution of the intensity of the oxidized products extracted from the mass chromatograms registered for the corresponding specific masses.

The XIC for the ion at m/z 830 corresponding to [M + 3O] revealed the formation of several products (Figure 4c). The main peak was assigned to a hydroxy hydroperoxide derivative, according to the LC−MS/MS analysis (data not shown). Its intensity increased in the first minutes of irradiation and then slowly decreased. Another product was assigned to a trihydroxy derivative, whose peak intensity slightly increased with the irradiation time.

Similar experiments were performed using Ptr as a photosensitizer. The MS analysis of the products showed that the rate of the overall oxidation of DLPC was much slower than that observed when *O*-decyl-Ptr is used as a photosensitizer, which is in agreement with the results shown in the previous section. Controls without the photosensitizer showed that the rate of oxidation was even slower than that registered when Ptr is used as the photosensitizer.

DOI: 10.1021/acs.langmuir.8b03302
Langmuir 2018, 34, 15578−15586

Scheme 1. Proposed Mechanism of Lipid Peroxidation by Photosensitization with *O*-Decyl-Ptr[a]

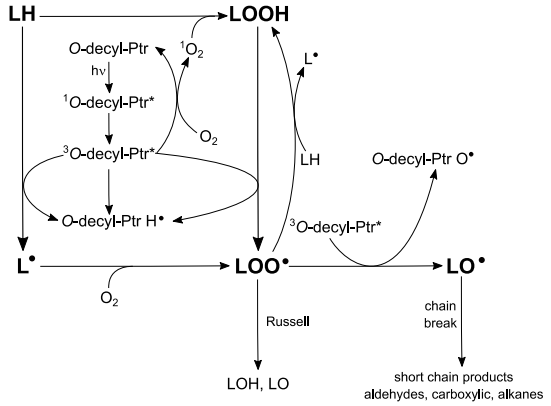

[a]LOOH, hydroperoxides; LH, phospholipids; L•, alkyl lipid radical; LOO•, peroxyl lipid radical; LO•, alkoxyl lipid radical; LOH, hydroxy derivatives; LO, carbonyl derivative.

Furthermore, LC−MS analysis also revealed the formation of products with molecular weights lower than that of the reactant. Several compounds with one of the fatty acids shorter than in DLPC were identified (Table 2). In particular, intense signals were detected for *m*/*z* values of 690.43 and 674.44 that correspond to 2-(9-carboxy-nonanoyl)−LPC and 2-(9-oxo-nonanoyl)−LPC, respectively. Analysis of the intensities of these chromatographic peaks of these compounds showed that their concentrations increased as a function of irradiation time (Figure 5). Taking into account previous studies on lipid peroxidation,[49,50] these phospholipid oxidation products are formed after rearrangement and cleavages of hydroxyl derivatives or LO• radicals, produced by reduction of hydroperoxides (Scheme 1).

In overview, the results presented in this section show that photosensitization of DLPC LUVs with *O*-decyl-Ptr led to the oxidation of unsaturated fatty acids yielding hydroperoxide and hydroxy derivatives which in turn undergo cleavage to form short-chain secondary products. A kinetic qualitative assessment of the formation of the different products, suggested that no accumulation of hydroperoxides took place before the production of hydroxy derivatives and short chain secondary products, which might indicate a fast photosensitized conversion of the former into the latter.

Photoinduced Membrane Damage. To study and compare membrane damage generated by the photosensitizers *O*-decyl-Ptr and Ptr, SoyPC LUVs containing the self-quenched fluorescent probe CF were irradiated during 50 min in the presence of both photosensitizers. As shown in Figure 6, Ptr produced almost no variation in CF fluorescence during irradiation, very similar to the control without the photosensitizer. On the contrary, the emission of CF at 517 nm rapidly increased when *O*-decyl-Ptr was present in LUVs, indicating that CF leakage through the membrane bilayer occurred. After 20 min of irradiation, *O*-decyl-Ptr reached the fluorescence detected after the complete disruption of SoyPC LUVs by the addition of Triton X-100, showing that nearly 100% of the CF leaked in the presence of *O*-decyl-Ptr (see eq 4). For the same irradiation time (20 min), with Ptr or in the absence of the photosensitizer, SoyPC LUVs showed CF released around only 5%. Dark control experiments showed no release of CF.

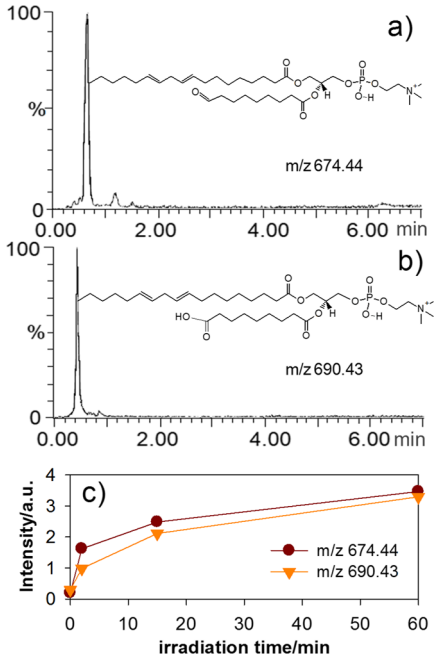

Figure 5. Extracted ion LC−MS chromatograms from short-chain products and their structure (a) *m*/*z* 674.44 and (b) *m*/*z* 690.43. (c) Time evolution of the intensity of the two short-chain products extracted from the mass chromatograms registered for the corresponding specific masses.

DLPC GUVs were irradiated in the presence of a given photosensitizer (5 μM) and simultaneously observed under an optical microscope in phase contrast mode (Figure 7). When *O*-decyl-Ptr was used, the optical contrast fades in less than 5 min of continuous irradiation. Such contrast loss is related to sucrose/glucose exchange due to pore formation, thus reflecting an increase in membrane permeability as a membrane response to lipid photo-oxidation. Noteworthy,

Table 2. Molecular Formula, Observed and Calculated Mass and Mass Error of DLPC Short-Chain Secondary Products Detected in LC−MS Spectra[a]

	molecular formula	observed mass	calculated mass	error (ppm)	error (mDa)
2-(8-oxo-octanoyl)−LPC	$C_{34}H_{63}NO_9P^+$	660.4242	660.4240	0.2	0.1
2-(9-oxo-nonanoyl)−LPC	$C_{35}H_{65}NO_9P^+$	674.4406	674.4397	1.4	0.9
2-(9-carboxy-nonanoyl)−LPC	$C_{35}H_{65}NO_{10}P^+$	690.4337	690.4346	−1.3	−0.9
2-(11-oxo-9-undecenoyl)−LPC	$C_{37}H_{67}NO_9P^+$	700.4551	700.4553	−0.3	−0.2
2-(12-oxo-9-undecenoyl)−LPC	$C_{38}H_{69}NO_9P^+$	714.4713	714.4710	0.4	0.3
2-(9-hydroxy-12-carboxy-10-dodecenoyl)−LPC	$C_{38}H_{69}NO_{11}P^+$	746.4603	746.4608	−0.7	−0.5
2-(13-oxo-9,11-tridecedienoyl)−LPC	$C_{39}H_{69}NO_9P^+$	726.4716	726.4704	0.8	0.6

[a]LPC: linoleoyl-phosphocholine.

DOI: 10.1021/acs.langmuir.8b03302
Langmuir 2018, 34, 15578−15586

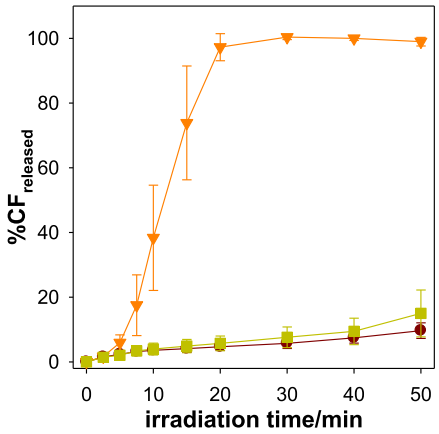

Figure 6. % $CF_{released}$ as a function of irradiation time using SoyPC LUVs with *O*-decyl-Ptr (orange down-pointing triangle), Ptr (yellow square) and without any photosensitizer (brown circle). Error bars correspond to SD from 3 different experiments.

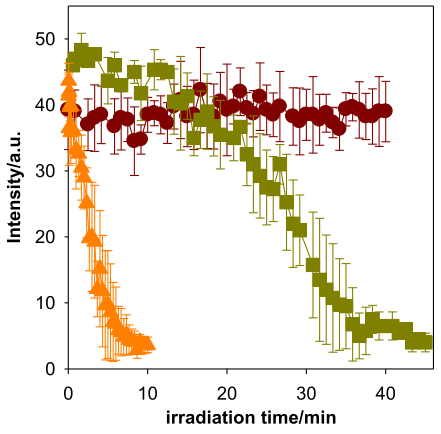

Figure 8. Profiles of contrast decay of DLPC GUVs with *O*-decyl-Ptr (orange up-pointing triangle), Ptr (green square) and without photosensitizer (brown circle). Each point corresponds to the average of atleast five vesicles and the SD is represented by the error bar.

neither microscaled pores nor membrane disruption were observed up to 1 h of continuous irradiation without the photosensitizer. On the other hand, the contrast fading was significantly slower for photo-irradiated GUVs dispersed in Ptr solutions. Figure 8 presents the profiles of brightness intensity decrease along the irradiation time for GUVs in the presence and absence of both photosensitizers. As shown in Figure 8, the loss of contrast using *O*-decyl-Ptr is quite faster compared with Ptr which took at least 20 min of irradiation before starting to lose contrast. Such effect is in line with the CF-release from LUVs described above.

Therefore, our results performed with both LUVs and GUVs clearly demonstrate that irradiation of phospholipid vesicles with *O*-decyl-Ptr leads to a fast increase in the permeability of the membrane, revealing a high efficiency of the alkyl-pterin to photoinduce lipid membrane damage. It is also worth mentioning that the interaction of *O*-decyl-Ptr with the biomembranes because of the presence of the alkyl side chain dramatically favors the photoinduced increase of permeability when compared with experiments performed with Ptr. This is in agreement with the fact that the formation of oxidized products was much faster using *O*-decyl-Ptr than Ptr in solution, as described in previous sections.

It is well known that oxidation of the double bond(s) on the acyl tails(s) of the unsaturated phospholipids promotes lipid hydroperoxidation (Scheme 1).[51] When hydroperoxide species accumulate in the membrane, large membrane fluctuations ending in surface area increase were reported with no increase in membrane permeability.[11,12,52] In contrast, pore formation is observed when oxidized lipids with shortened chains are present in the biomembrane.[53,54] In particular, it has been recently predicted by molecular dynamic simulations that the presence of a significant amount of oxidized lipids hanging aldehydes and carboxylic groups in the end of the truncated chains promote membrane pore formation.[55]

In the current work, the significant increase in membrane permeability in LUVs and GUVs experiments is consistent with the detection of shortened oxidized lipids evidenced by MS (Table 2, Figure 5). However, neither membrane fluctuations nor area increase preceded membrane contrast fading (Figure 8), suggesting there is no hydroperoxide accumulation in agreement with our MS data (Table 1). Therefore, our combined results give support to the conclusion that lipid hydroperoxides formed by pterin-derivatives photosensitized oxidation do not accumulate in membrane, but the oxidation pathway is such that oxidized lipids with shortened chains are preferred to accumulate in the membrane than hydroperoxides as schematically represented in Scheme 1. Although similar profile of lipid peroxidation products was observed for DO15,[17] a major difference is that this PDT photosensitizer leads to the increased accumulation of lipid hydroperoxides, while in the case of *O*-decyl-Ptr lipid hydroperoxides do not accumulate. This is likely to represent differences in terms of membrane insertion and in the competition between type I and type II mechanisms for phenothiazinium cations compared with pterin derivatives. Indeed, the electronic structure of pterins favors contact-dependent non-covalent interactions with biological targets and consequently the role of the type I process in photosensitized oxidations usually overrules that of type II.

CONCLUSIONS

In this work, we show that the lipophilic pterin derivative, namely, 4-(decyloxy)pteridin-2-amine (*O*-decyl-Ptr), is capable of photosensitizing the oxidation of lipid membranes upon UVA irradiation. Unilamellar vesicles of phosphatidylcholine

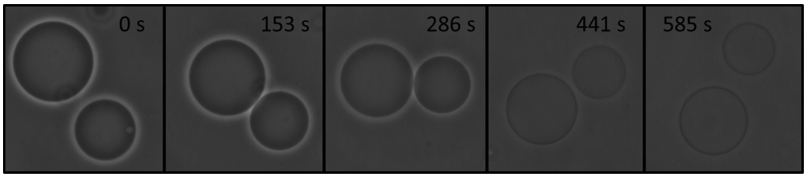

Figure 7. Phase contrast optical microscopy of time running sequences (in seconds) of the damage on DLPC GUVs by photosensitization with *O*-decyl-Ptr (5 μM).

DOI: 10.1021/acs.langmuir.8b03302
Langmuir 2018, 34, 15578−15586

rich in PUFAs were used as model biomembranes. We also show that *O*-decyl-Ptr is more efficient at the photosensitized oxidation of lipids compared to Ptr, the unsubstituted derivative of the pterin family. In particular, pterin freely passes across lipid membranes, whereas *O*-decyl-Ptr, because of its alkyl chain, intercalates in the lipid bilayer.

Lipid peroxidation photosensitized by *O*-decyl-Ptr led to the formation of conjugated dienes and oxidized lipids, such as hydroxyl derivatives, hydroperoxides, and hydroxyhydroperoxides. These photoproducts undergo a fast conversion into short-chain secondary products by cleavage of the fatty acid chains most likely due to further photosensitized processes that convert the peroxyl lipid radicals into the corresponding alkoxyl lipid radicals. The formation of short-chain oxidized lipids thus imparts on the phospholipid bilayer structure promoting membrane leakage. In this way, our results furnish a valuable information regarding the photodynamic mechanism of action of *O*-decyl-Ptr in biomembranes which, in turn, may perturb cell homeostasis and trigger cell death.

AUTHOR INFORMATION

Corresponding Authors

*E-mail: itri@if.usp.br (R.I.).
*E-mail: athomas@inifta.unlp.edu.ar (A.H.T.).

ORCID

Alexander Greer: 0000-0003-4444-9099
Mauricio S. Baptista: 0000-0001-7079-7666
Andrés H. Thomas: 0000-0002-8054-7799

Notes

The authors declare no competing financial interest.

ACKNOWLEDGMENTS

This work was partially supported by Agencia de Promoción Científica y Tecnológica (ANPCyT-grants PICT 2012-0508 and 2015-1988), Universidad Nacional de La Plata (UNLP-grant X712), São Paulo Research Foundation (FAPESP, Process 2012/50680-5 and 2013/07937-8), National Science Foundation (NSF, CHE-1464975) and Portuguese National Funds (NORTE-01-0145-FEDER-000011). M.V. thanks FAPESP for the Visiting Researcher Grant (2016/04296-0). M.V., M.N.U., A.H.T. and A.G. thank Consejo Nacional de Investigaciones Científicas y Técnicas (CONICET) and NSF for supporting their collaboration through a Bilateral Cooperation Programme Level I. M.N.U. thanks CONICET for postdoctoral research fellowship. The authors gratefully acknowledge Niluksha Walalawela (Brooklyn College, CUNY) for his valuable help on the synthesis of *O*-decyl-Ptr and Nathalie Martins-Froment (Service Commun de Spectrométrie de Masse (FR2599), Université de Toulouse III (Paul Sabatier)) for her contribution in MS. R.I. and M.S.B. are recipients of The National Council for Scientific and Technological Development (CNPq, Brazil) research fellowship. M.V. and A.H.T. are research members of CONICET.

ABBREVIATIONS

Ptr, pterin; *O*-decyl-Ptr, 4-(decyloxy)pteridin-2-amine; PUFAs, polyunsaturated fatty acids; LUVs, large unilamellar vesicles; GUVs, giant unilamellar vesicles; CF, 5(6)-carboxyfluorescein; SoyPC, L-α-soybean phosphatidylcholine; DLPC, 1,2-dilinoleoyl-*sn*-glycero-3-phosphocholine; DOPC, 1,2-dioleoyl-*sn*-glycero-3-phosphocholine

REFERENCES

(1) Repetto, M.; Semprine, J.; Boveris, A. Lipid Peroxidation: Chemical Mechanism, Biological Implications and Analytical Determination. *Lipid Peroxidation*; INTECH, 2012.
(2) Girotti, A. W. Lipid hydroperoxide generation, turnover, and effector action in biological systems. *J. Lipid Res.* **1998**, *39*, 1529−1542.
(3) Reis, A. Oxidative Phospholipidomics in health and disease: Achievements, challenges and hopes. *Free Radical Biol. Med.* **2017**, *111*, 25−37.
(4) Bonnett, R. *Chemical Aspects of Photodynamic Therapy*; Gordon and Breach Science Publishers: Amsterdam, The Netherlands, 2000.
(5) Dougherty, T. J.; Gomer, C. J.; Henderson, B. W.; Jori, G.; Kessel, D.; Korbelik, M.; Moan, J.; Peng, Q. Photodynamic therapy. *J. Natl. Cancer Inst.* **1998**, *90*, 889−905.
(6) Hamblin, M. *Advances in Photodynamic Therapy: Basic*; Translational And Clinical Artech House, Inc: Norwood, MA, 2008.
(7) Baptista, M. S.; Cadet, J.; Di Mascio, P.; Ghogare, A. A.; Greer, A.; Hamblin, M. R.; Lorente, C.; Nunez, S. C.; Ribeiro, M. S.; Thomas, A. H.; Vignoni, M.; Yoshimura, T. M. Type I and II Photosensitized Oxidation Reactions: Guidelines and Mechanistic Pathways. *Photochem. Photobiol.* **2017**, *93*, 912−919.
(8) Foote, C. S. Definition of Type I and Type II photosensitized oxidation. *Photochem. Photobiol.* **1991**, *54*, 659.
(9) Calori, I. R.; Tedesco, A. C. Lipid vesicles loading aluminum phthalocyanine chloride: Formulation properties and disaggregation upon intracellular delivery. *J. Photochem. Photobiol., B* **2016**, *160*, 240−247.
(10) Ytzhak, S.; Bernstein, S.; Loew, L. M.; Ehrenberg, B. The correlation between photosensitizers' membrane localization, membrane-residing targets and photosensitization efficiency. *Progress in Biomedical Optics and Imaging−Proceedings of SPIE*, 2009.
(11) Riske, K. A.; Sudbrack, T. P.; Archilha, N. L.; Uchoa, A. F.; Schroder, A. P.; Marques, C. M.; Baptista, M. S.; Itri, R. Giant Vesicles under Oxidative Stress Induced by a Membrane-Anchored Photosensitizer. *Biophys. J.* **2009**, *97*, 1362−1370.
(12) Weber, G.; Charitat, T.; Baptista, M. S.; Uchoa, A. F.; Pavani, C.; Junqueira, H. C.; Guo, Y.; Baulin, V. A.; Itri, R.; Marques, C. M.; Schroder, A. P. Lipid oxidation induces structural changes in biomimetic membranes. *Soft Matter* **2014**, *10*, 4241−4247.
(13) Lavi, A.; Weitman, H.; Holmes, R. T.; Smith, K. M.; Ehrenberg, B. The Depth of Porphyrin in a Membrane and the Membrane's Physical Properties Affect the Photosensitizing Efficiency. *Biophys. J.* **2002**, *82*, 2101−2110.
(14) Mojzisova, H.; Bonneau, S.; Maillard, P.; Berg, K.; Brault, D. Photosensitizing properties of chlorins in solution and in membrane-mimicking systems. *Photochem. Photobiol. Sci.* **2009**, *8*, 778−787.
(15) Wang, H.-J.; Liang, R.; Du, H.-H.; Ai, J.-X.; Han, R.-M.; Zhang, J.-P.; Skibsted, L. H. Riboflavin and chlorophyll as photosensitizers in electroformed giant unilamellar vesicles as food models. *Eur. Food Res. Technol.* **2017**, *243*, 21−26.
(16) Matsumoto, J.; Suemoto, Y.; Kanemaru, H.; Takemori, K.; Shigehara, M.; Miyamoto, A.; Yokoi, H.; Yasuda, M. Alkyl substituent effect on photosensitized inactivation of Escherichia coli by pyridinium-bonded P-porphyrins. *J. Photochem. Photobiol., B* **2017**, *168*, 124−131.
(17) Bacellar, I. O. L.; Oliveira, M. C.; Dantas, L. S.; Costa, E. B.; Junqueira, H. C.; Martins, W. K.; Durantini, A. M.; Cosa, G.; Di Mascio, P.; Wainwright, M.; Miotto, R.; Cordeiro, R. M.; Miyamoto, S.; Baptista, M. S. Photosensitized Membrane Permeabilization Requires Contact-Dependent Reactions between Photosensitizer and Lipids. *J. Am. Chem. Soc.* **2018**, *140*, 9606−9615.
(18) Brown, D. J. Fused Pyrimidines: Pteridines. *The Chemistry of Heterocyclic Compounds*; John Wiley & Sons: New York, 1988; Vol. *24*, pp 1−42.
(19) Pfleiderer, W. Natural pteridines-A chemical hobby. In *Chemistry and Biology of Pteridines and Folates*; Ayling, J. E., Gopal Nair, M., Baugh, C. M., Eds.; Plenum Press: New York, 1993; Vol. *338*, pp 1−16.

DOI: 10.1021/acs.langmuir.8b03302
Langmuir 2018, 34, 15578−15586

(20) Kappock, T. J.; Caradonna, J. P. Pterin-dependent amino acid hydroxylases. *Chem. Rev.* **1996**, *96*, 2659−2756.
(21) Ziegler, I. Production of pteridines during hematopoiesis and T-lymphocyte proliferation: Potential participation in the control of cytokine signal transmission. *Med. Res. Rev.* **1990**, *10*, 95−114.
(22) Schallreuter, K.; Wood, J.; Pittelkow, M.; Gutlich, M.; Lemke, K.; Rodl, W.; Swanson, N.; Hitzemann, K.; Ziegler, I. Regulation of melanin biosynthesis in the human epidermis by tetrahydrobiopterin. *Science* **1994**, *263*, 1444−1446.
(23) Lorente, C.; Thomas, A. H. Photophysics and photochemistry of pterins in aqueous solution. *Acc. Chem. Res.* **2006**, *39*, 395−402.
(24) Rokos, H.; Beazley, W. D.; Schallreuter, K. U. Oxidative stress in vitiligo: Photo-oxidation of pterins produces H_2O_2 and pterin-6-carboxylic acid. *Biochem. Biophys. Res. Commun.* **2002**, *292*, 805−811.
(25) Reid, L. O.; Roman, E. A.; Thomas, A. H.; Dántola, M. L. Photooxidation of Tryptophan and Tyrosine Residues in Human Serum Albumin Sensitized by Pterin: A Model for Globular Protein Photodamage in Skin. *Biochemistry* **2016**, *55*, 4777−4786.
(26) Hirakawa, K.; Suzuki, H.; Oikawa, S.; Kawanishi, S. Sequence-specific DNA damage induced by ultraviolet A-irradiated folic acid via its photolysis product. *Arch. Biochem. Biophys.* **2003**, *410*, 261−268.
(27) Serrano, M. P.; Vignoni, M.; Lorente, C.; Vicendo, P.; Oliveros, E.; Thomas, A. H. Thymidine radical formation via one-electron transfer oxidation photoinduced by pterin: Mechanism and products characterization. *Free Radical Biol. Med.* **2016**, *96*, 418−431.
(28) Serrano, M. P.; Estébanez, S.; Vignoni, M.; Lorente, C.; Vicendo, P.; Oliveros, E.; Thomas, A. H. Photosensitized oxidation of 2′-deoxyguanosine 5′-monophosphate: mechanism of the competitive reactions and product characterization. *New J. Chem.* **2017**, *41*, 7273−7282.
(29) Dántola, M. L.; Zurbano, B. N.; Thomas, A. H. Photoinactivation of tyrosinase sensitized by folic acid photoproducts. *J. Photochem. Photobiol., B* **2015**, *149*, 172−179.
(30) Miñán, A.; Lorente, C.; Ipiña, A.; Thomas, A. H.; de Mele, M. F. L.; Schilardi, P. L. Photodynamic inactivation induced by carboxypterin: a novel non-toxic bactericidal strategy against planktonic cells and biofilms of Staphylococcus aureus. *Biofouling* **2015**, *31*, 459−468.
(31) Thomas, A. H.; Catalá, Á.; Vignoni, M. Soybean phosphatidylcholine liposomes as model membranes to study lipid peroxidation photoinduced by pterin. *Biochim. Biophys. Acta, Biomembr.* **2016**, *1858*, 139−145.
(32) Vignoni, M.; Walalawela, N.; Bonesi, S. M.; Greer, A.; Thomas, A. H. Lipophilic Decyl Chain−Pterin Conjugates with Sensitizer Properties. *Mol. Pharm.* **2018**, *15*, 798−807.
(33) Walalawela, N.; Vignoni, M.; Urrutia, M. N.; Belh, S. J.; Greer, E. M.; Thomas, A. H.; Greer, A. Kinetic Control in the Regioselective Alkylation of Pterin Sensitizers: A Synthetic, Photochemical, and Theoretical Study. *Photochem. Photobiol.* **2018**, *94*, 834−844.
(34) Serrano, M. P.; Vignoni, M.; Dántola, M. L.; Oliveros, E.; Lorente, C.; Thomas, A. H. Emission properties of dihydropterins in aqueous solutions. *Phys. Chem. Chem. Phys.* **2011**, *13*, 7419−7425.
(35) Kuhn, H. J.; Braslavsky, S. E.; Schmidt, R. Chemical actinometry (IUPAC technical report). *Pure Appl. Chem.* **2004**, *76*, 2105−2146.
(36) Angeli, N. G.; Lagorio, M. G.; Román, E. A. S.; Dicelio, L. E. Meso-Substituted Cationic Porphyrins of Biological Interest. Photophysical and Physicochemical Properties in Solution and Bound to Liposomes. *Photochem. Photobiol.* **2007**, *72*, 49−56.
(37) Wolff, S. P. Ferrous ion oxidation in presence of ferric ion indicator xylenol orange for measurement of hydroperoxides. *Methods Enzymol.* **1994**, *233*, 182−189.
(38) Martins, R. M.; Amino, R.; Daghastanli, K. R.; Cuccovia, I. M.; Juliano, M. A.; Schenkman, S. A short proregion of trialysin, a pore-forming protein of Triatomainfestans salivary glands, controls activity by folding the N-terminal lytic motif. *FEBS J.* **2008**, *275*, 994−1002.
(39) Weinstein, J.; Yoshikami, S.; Henkart, P.; Blumenthal, R.; Hagins, W. Liposome-cell interaction: transfer and intracellular release of a trapped fluorescent marker. *Science* **1977**, *195*, 489−492.
(40) Angelova, M. I.; Dimitrov, D. S. Liposome electroformation. *Faraday Discuss. Chem. Soc.* **1986**, *81*, 303−311.
(41) Bligh, E. G.; Dyer, W. J. A rapid method of total lipid extraction and purification. *Can. J. Biochem. Physiol.* **1959**, *37*, 911−917.
(42) Ehrenberg, B.; Gross, E. The effect of liposomes' membrane composition on the binding of the photosensitizers Hpd and photofrin II. *Photochem. Photobiol.* **1988**, *48*, 461−466.
(43) Frankel, E. N.; Huang, S.-W.; Prior, E.; Aeschbach, R. Evaluation of Antioxidant Activity of Rosemary Extracts, Carnosol and Carnosic Acid in Bulk Vegetable Oils and Fish Oil and Their Emulsions. *J. Sci. Food Agric.* **1996**, *72*, 201−208.
(44) Novak, F.; Borovska, J.; Vecka, M.; Rychlikova, J.; Vavrova, L.; Petraskova, H.; Zak, A.; Novakova, O. Plasma Phospholipid Fatty Acid Profile is Altered in Both Septic and Non-Septic Critically Ill: A Correlation with Inflammatory Markers and Albumin. *Lipids* **2017**, *52*, 245−254.
(45) White, C. R.; Brock, T. A.; Chang, L. Y.; Crapo, J.; Briscoe, P.; Ku, D.; Bradley, W. A.; Gianturco, S. H.; Gore, J.; Freeman, B. A. Superoxide and peroxynitrite in atherosclerosis. *Proc. Natl. Acad. Sci. U.S.A.* **1994**, *91*, 1044−1048.
(46) Stewart, J. C. M. Colorimetric determination of phospholipids with ammonium ferrothiocyanate. *Anal. Biochem.* **1980**, *104*, 10−14.
(47) Serrano, M. P.; Lorente, C.; Borsarelli, C. D.; Thomas, A. H. Unraveling the Degradation Mechanism of Purine Nucleotides Photosensitized by Pterins: The Role of Charge-Transfer Steps. *ChemPhysChem* **2015**, *16*, 2244−2252.
(48) Reis, A.; Domingues, M. R. M.; Amado, F. M. L.; Ferrer-Correia, A. J.; Domingues, P. Radical peroxidation of palmitoyl-lineloyl-glycerophosphocholine liposomes: Identification of long-chain oxidised products by liquid chromatography-tandem mass spectrometry. *J. Chromatogr. B: Anal. Technol. Biomed. Life Sci.* **2007**, *855*, 186−199.
(49) Reis, A.; Spickett, C. M. Chemistry of phospholipid oxidation. *Biochim. Biophys. Acta, Biomembr.* **2012**, *1818*, 2374−2387.
(50) Khoury, S.; Pouyet, C.; Lyan, B.; Pujos-Guillot, E. Evaluation of oxidized phospholipids analysis by LC-MS/MS. *Anal. Bioanal. Chem.* **2018**, *410*, 633−647.
(51) Niki, E. Lipid peroxidation: Physiological levels and dual biological effects. *Free Radical Biol. Med.* **2009**, *47*, 469−484.
(52) Wong-ekkabut, J.; Xu, Z.; Triampo, W.; Tang, I.-M.; Tieleman, D. P.; Monticelli, L. Effect of Lipid Peroxidation on the Properties of Lipid Bilayers: A Molecular Dynamics Study. *Biophys. J.* **2007**, *93*, 4225−4236.
(53) Caetano, W.; Haddad, P. S.; Itri, R.; Severino, D.; Vieira, V. C.; Baptista, M. S.; Schröder, A. P.; Marques, C. M. Photo-Induced Destruction of Giant Vesicles in Methylene Blue Solutions. *Langmuir* **2007**, *23*, 1307−1314.
(54) Runas, K. A.; Malmstadt, N. Low levels of lipid oxidation radically increase the passive permeability of lipid bilayers. *Soft Matter* **2015**, *11*, 499−505.
(55) Boonnoy, P.; Jarerattanachat, V.; Karttunen, M.; Wong-ekkabut, J. Bilayer Deformation, Pores, and Micellation Induced by Oxidized Lipids. *J. Phys. Chem. Lett.* **2015**, *6*, 4884−4888.

DOI: 10.1021/acs.langmuir.8b03302
Langmuir 2018, 34, 15578−15586